

Geometrical Characteristics and Reactivities of Tetracoordinated Pd Complexes: Mono- and Bidentate Ligands and Charged and Uncharged Ligands

Jin-seon Yoo, Dong-su Ha, Jae Sang Kim,[†] Bong Gon Kim,[‡] and Jong Keun Park^{‡,*}

Department of Physical Chemistry, The Graduate School of Education, Suncheon National University, Suncheon 660-701, Korea

[†]Department of Chemistry, Research Institute of Natural Science, Graduate School for Molecular Materials and Nanochemistry, Gyeongsang National University, Jinju 660-701, Korea

[‡]Department of Chemistry Education, Research Institute of Natural Science, and Educational Research Institute, Gyeongsang National University, Jinju 660-701, Korea. *E-mail: mc7@gnu.ac.kr

Received January 2, 2008

The geometrical structures, atomic charges, and relative energies of tetracoordinated Pd complexes [PdCl₃Z (Z = Cl⁻, Br⁻, OH⁻, H₂O, NH₃, PH₃), PdCl₂Z₂ (Z = Br⁻, OH⁻, H₂O, NH₃, PH₃), PdZ₂X (Z = Cl⁻, OH⁻, H₂O, NH₃, PH₃; X = oxalate, O₂⁻CCO₂⁻), and PdZ₂Y (Z = Cl⁻, OH⁻, H₂O, NH₃, PH₃; Y = succinate, CO₂⁻CHCHCO₂⁻)] and the ligand exchange reactions of the Pd complexes were investigated using the *ab initio* second order Möller-Plesset perturbation (MP2) and Density Functional Theory (DFT) methods. The geometrical characteristics of the tetracoordinated Pd(II) complexes with mono- and bidentate ligands, the effects of the atomic charges for the charged and uncharged ligands, the (d_{z²}-π) interactions between the d_{z²}-orbital of Pd(II) and the π-orbital of bidentates, and the relative stabilities between the isomers of PdCl₂Z₂ and PdZ₂Y were investigated in detail. The potential energy surfaces for the ligand exchange reactions used for the conversions of {[PdCl₂(NH₃)₂] + H₂O} to {[PdCl(NH₃)₂(H₂O)]⁺ + Cl⁻} and {[PdCl₂(PH₃)₂] + H₂O} to {[PdCl(PH₃)₂(H₂O)]⁺ + Cl⁻} were investigated. The geometrical structure variations, molecular orbital variations (HOMO and LUMO), and relative stabilities for the ligand exchange processes were also examined quantitatively.

Key Words : Geometrical structures, Potential energy surfaces, Ligand exchange reactions, Atomic charge, Density functional theory

Introduction

The properties and reactivities of palladium complexes have been studied with various theoretical and experimental techniques.¹⁻¹² In particular, the reactivities have been investigated by focusing on the geometrical structures (PdL₄, PdL₅, PdL₆) and the ligand exchange reactions in the solvation system *via* a ligand-solvent interaction and/or metal-solvent/ligand interaction (*e.g.*, Pd-DNA bases interactions).¹⁻³ In the tetracoordinated Pd(II) complexes, the ground electronic configuration of the central Pd(II) metal is 4d⁸ with a partially occupied d-shell as a ³F state. Since the unoccupied d_{x²-y²} orbital of the Pd center interacts with the lone pair orbitals of four surrounding ligands, the structural characteristic of Pd(II) complexes has the tendency to form square planar geometry. The occupied d_{z²}-orbital of Pd(II) interacts with the fifth or sixth ligands at the axial positions of the square planar geometry.^{3,4}

The binding between the transition metal and macrocyclic ligands containing electronegative atoms are formed with the coordination of the N- and O-atoms (hard σ-donor properties) and the P- and S-atoms (soft σ-donor and π-acceptor properties) on the ligand.¹⁻⁴ The geometrical structures of the macrocyclic Pd complexes are distorted from the π-acceptor property using empty d-orbitals on the P- and S-atom. Generally, the Pd(II) complexes have a square-planar Pd(II) center bound to the electronegative atom on ligands. With the presence of an axial (Pd···L) intra-molecular

interaction, the geometrical structure of the macrocyclic Pd complexes {Pd([9]aneS₂O)Cl₂} results in five coordinated complexes. The Pd(II) center is not co-planar with the four donor set. Two of the donor atoms lie above the mean plane and two atoms below.⁴ The distances of the apical (Pd···L) interaction are longer than the values of a Pd-S (Pd-N, Pd-O) bond observed normally.^{1,2} That is, the distance (2.92 Å) of the axial (Pd···S) interaction is in excess of the normal bonding range of R_(Pd-S) = (2.30~2.50 Å). Meanwhile, the Pd-S distances of the two equatorial thia donors are shorter than those of Pd(II) complexes coordinated with four equatorial thia donors.^{1,2} Regarding the decrease of the Pd-S distances, it has been known that π-orbital back donation occurs from the Pd(II) ion to the S atom. The characteristics of the microcyclic-metal complexes are electronically controlled by the metal-donor atom interactions rather than by any conformational and configurational constraints of the macrocyclic ligands.

The ligand exchange reactions at the Pd(II) center are suggested to proceed *via* a five-coordinated metal-ligand interaction.⁵⁻¹¹ These ligand exchange processes are also characterized by electron density transfers from the entering ligands with the lone pair electron to the leaving L groups *via* the central Pd(II) metal. In the reaction mechanisms associated with the ligand exchanges at the Pd(II) complexes, the exchange reaction proceeds *via* a vertically five-coordinated transition state ([PdL₅][‡]) leading to C_{2v}-symmetry.⁵ The relative activation energies for the exchange

reactions are about 3–49 kJ/mol. The geometrical structures and potential energy surfaces for the ligand exchange reactions of the platinum complexes were examined by Park *et al.*^{9,10} The transition state for the exchange reactions has a C_1 -symmetrical structure with both hydrogen-bonded and direct metal-solvent interactions. The hydrolysis processes of *cis*-dichloro(ethylenediamine)platinum were investigated by Santos group.⁸ In the reactant and product, the entering H_2O and leaving Cl groups hydrogen-bond to the central Pt cation. In the transition state, the oxygen atom of the entering water axially bonds to the d_{z^2} -orbital of Pt(II) and two H atoms of the water simultaneously orient towards the two chloride. Experimentally,^{11,12} two vertical metal-oxygen interactions at the apical positions of the square planar $PtCl_4^{2-}$ complexes were observed by Caminiti *et al.*¹¹ The geometrical structure of $[MCl_4]^{2-} \cdot (H_2O)_2$ by the metal-oxygen interaction is a distorted octahedral complex.

In this work, we studied the geometrical structures of the tetracoordinated Pd(II) complexes coordinated by the mono- and bidentate ligands and the potential energy curves of the ligand exchange reaction *via* a five-coordinated Pd-OH₂ interaction. First, the geometrical structures of the Pd(II) complexes were optimized with the monodentates and bidentates (neutral and anionic states). Second, the binding intensity of the N-, O- (σ -donor), and P-atom (σ -donor and π -acceptor) on the ligand and the fifth axial (Pd $\cdots\pi$ -orbital) interactions between Pd and the π -orbital of bidentate were examined. Finally, to elucidate the reactivities of the ligand exchange process in the ligand-solvent interaction and the interaction between Pd(II) and the fifth ligand, the potential energy surfaces of the conversion from the reactants (PdY₂L₂ + L') to the product (PdY₂LL' + L) were calculated.

Computational Methods

The equilibrium geometrical structures of tetracoordinated palladium [PdCl₃Z (Z = Cl⁻, Br⁻, OH⁻, H₂O, NH₃, PH₃), PdCl₂Z₂ (Z = Br⁻, OH⁻, H₂O, NH₃, PH₃), PdZ₂X (Z = Cl⁻, OH⁻, H₂O, NH₃, PH₃; X = oxalate, O₂⁻CCO₂⁻), and PdZ₂Y (Z = Cl⁻, OH⁻, H₂O, NH₃, PH₃; Y = succinate, CO₂⁻CHCHCO₂⁻)] complexes were fully optimized with the *ab initio* second-order Møller-Plesset perturbation (MP2), and density functional theory (DFT) levels using the Gaussian 03.^{13–15} The hybrid DFT (B1LYP, B3LYP, B3P86) density functional utilizes the exchange functional of Becke¹⁴ in conjunction with Lee-Yang-Parr correlation function¹⁵ and provides good structural and energy-related information, even for relatively large chemical systems such as transition metal complexes. To confirm the existence of stable structures, the harmonic vibrational frequencies of the species were analyzed at the B3P86 level. In addition, the atomic charges of the natural bond orbital (NBO) of the equilibrium (PdY₂L₂) complexes were also analyzed to investigate the charge transfer of the ligand exchanges. The standard 6-311+G** basis sets are used for the (H, N, O, P, Cl, and Br) atoms (3-21G** for Pd). To obtain more reasonable results, we used the lanl2dz basis functions for Pd.

The potential energy surfaces of the ligand exchange reactions from (PdZ₂Cl₂ + H₂O; Z = NH₃, PH₃) to (PdZ₂ClH₂O + Cl⁻) are calculated for R_{Pd-Cl} and R_{Pd-O} using the B3P86/(6-311+G** for H, N, O, P, Cl, Br; 3-21G** for Pd) levels. The potential energy curves from [Pd(NH₃)₂Cl₂ + H₂O] to [Pd(NH₃)₂Cl(OH₂) + Cl⁻] are calculated using the total energies as a function of the (Pd-O) distances in the range of 2.0 to 4.5 Å and the (Pd-Cl) distances in the range of 2.3 to 4.85 Å. The potential curves from [Pd(PH₃)₂Cl₂ + H₂O] to [Pd(PH₃)₂Cl(OH₂) + Cl⁻] are calculated using the total energies as a function of the (Pd-O) distances in the range of 2.0 to 4.5 Å and the (Pd-Cl) distances in the range of 2.3 to 4.5 Å.

Results and Discussion

Geometrical structures of Pd complexes. Geometrical structures of tetracoordinated Pd complexes at the B3P86/6-311+G** (3-21G** for Pd) level were optimized and the most stable isomers are represented in Figure 1. The geometrical structures used the lanl2dz basis functions for Pd are similar to those used 3-21G**. In the PdCl₃Z and PdCl₂Z₂ complexes, Pd(II) is located at the center of the square planar structure surrounded by four neutral and anionic ligands. The geometry of [PdCl₄]²⁻ is a D_{4h}-structure. Changing from one ligand to two, the geometrical structures of PdCl₃Z and PdCl₂Z₂ turn to C₁-symmetry. In the PdCl₂Z₂ complexes, the structures of the *trans*-types are more symmetric than those of the *cis*-type. In [PdCl₃Z, PdCl₂Z₂ (Z = OH⁻, NH₃, H₂O)], a type of 4-membered (Pd-Z-H \cdots Cl) interaction (the weakly long range interactions of R_{H \cdots O} = 2.2–2.4 Å) is formed and the optimized structures are slightly distorted. In particular, the structures of [PdCl₃(OH)]²⁻ and [PdCl₂(OH)₂]²⁻ with the anionic (OH⁻) ligand are more distorted than the others.

To investigate the (d_{z^2} - π) intra-molecular interaction, the geometrical structures of [PdZ₂(oxalate)] and [PdZ₂(succinate)] coordinated with the bidentate were optimized. The oxalate (O₂⁻CCO₂⁻) is a bidentate ligand consisting of an ethylene unit and four oxygen atoms. When a oxalate coordinates to Pd(II), the *cis*-[PdZ₂(oxalate)] complexes with a 5-membered ring are optimized to be stable. Due to the short internuclear distance between the Pd atom and the ethylene group and the narrow coordinated angle, the twisted *cis*-[PdZ₂(oxalate)] complexes are not optimized except for twisted *cis*-[Pd(PH₃)₂(oxalate)], which exhibits the tetrahedral geometry. The structure of *cis*-[PdZ₂(oxalate)] is a completely planar geometry. In *cis*-[PdZ₂(oxalate) (Z = OH⁻, NH₃, H₂O)], the H atom of Z directs to the lone pair electron of the binding O atom in oxalate.

To reduce the repulsion owing to the short distance between Pd(II) and the ligand, the succinate is chosen as a bidentate ligand. The succinate (CO₂⁻CHCHCO₂⁻) ligand consists of an ethylene unit and two carboxylate groups. When a succinate coordinates to Pd(II), a 7-membered ring in the Pd complex is formed. The internuclear distance between the Pd(II) center and the C=C group in [PdZ₂(succinate)] is slightly longer than that of [PdZ₂(oxalate)]. As a

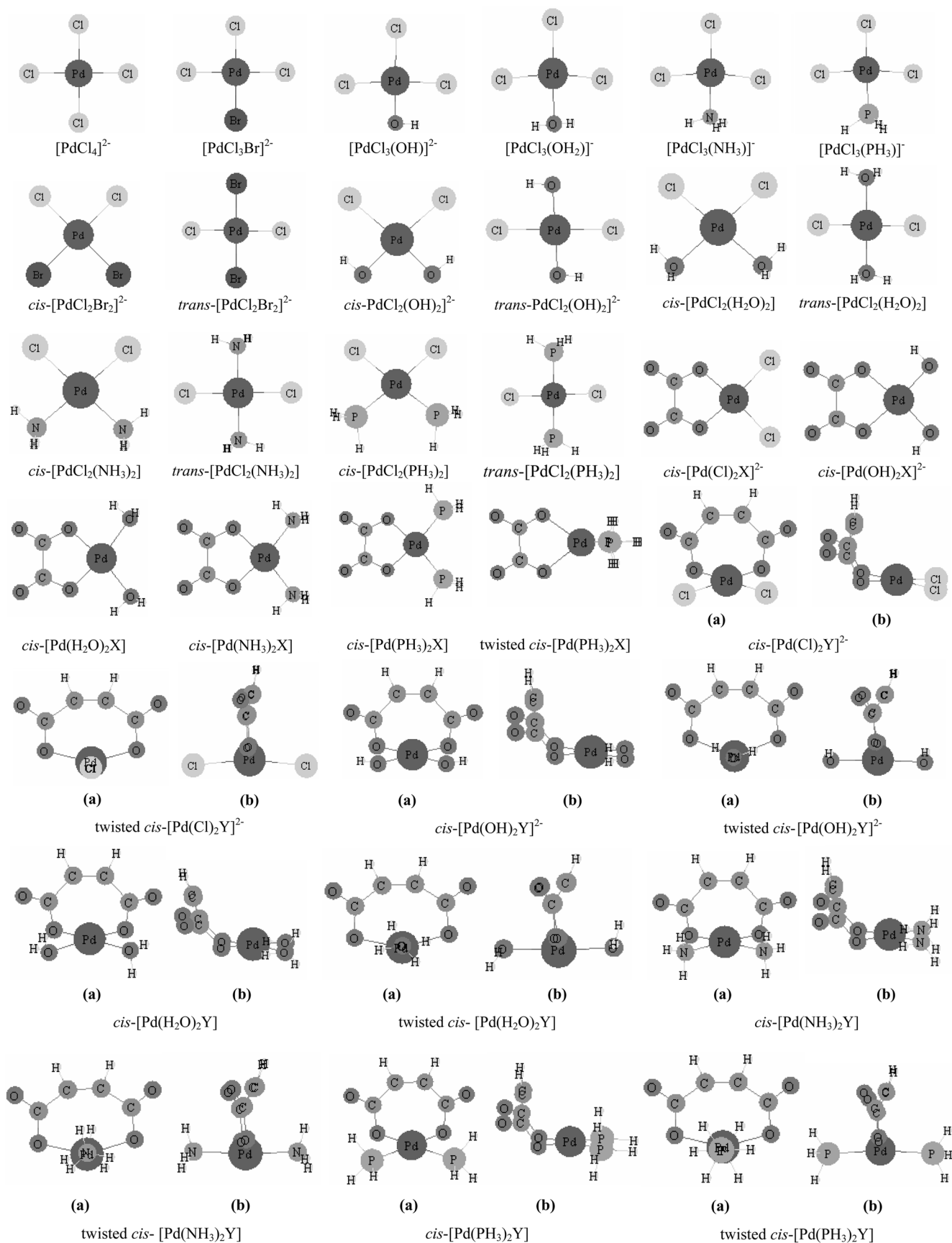


Figure 1. Optimized geometrical structures of $[PdCl_3Z]$, $[PdCl_2Z_2]$, $[PdZ_2X]$, and $[PdZ_2Y]$ at the B3P86/6-311+G** (3-21G** for Pd) levels. The frontal view denoted as (a), the side view denoted as (b).

results, the *cis*- and twisted *cis*-types of [PdZ₂(succinate)] are optimized to be stable as distorted square planar array. In *cis*-[PdZ₂(succinate)], the ethylene group of succinate localizes to the outer side on the square planar geometry. Therefore, the (π -d_{z²}) intra-molecular interaction between the π -orbital and the d_{z²}-orbital does not occur. On the other hand, in the twisted *cis*-[PdZ₂(succinate)], the ethylene group is located at the axial plane in parallel with the occupied d_{z²}-orbital of Pd. Due to the weakly (π -d_{z²}) intra-molecular repulsion, the structures of the twisted *cis*-[PdZ₂(succinate)] are not co-planar with the four donor atoms.

The parameters of the optimized structures of Pd complexes are listed in Table 1. Our optimized distances are slightly longer than those of the previous theoretical^{5,12,16-24} and experimental^{11,25-31} values. The obtained values used the lan12dz basis functions for Pd are similar to those used 3-21G^{**}. The internuclear (Pd-L) distances optimized at the B3P86 levels are shortest. In the dianionic [PdCl₃Z]²⁻ complexes coordinated with the anionic (Br⁻ and OH⁻) ligands, the (Pd-Br and Pd-OH) distances were relatively decreased with the interaction between the cation of Pd and the anion of the ligands. Therefore, the bond distances of R_{Pd-Cl}¹ of the *trans*-position are longer than R_{Pd-Cl}^c of the *cis*-position. Meanwhile, in PdCl₃Z with the neutral (NH₃, H₂O, PH₃) ligands, R_{Pd-Cl}¹ of the *trans*-position are shorter than R_{Pd-Cl}^c of the *cis*-position. Meanwhile, in [PdCl₂Z₂]²⁻ (Z = Br⁻, OH⁻), the R_{Pd-Cl} distances in *cis*-isomer are relatively longer than those of *trans*-isomer. By the long range (R_{H...Cl}) interaction in [PdCl₂(OH)₂]²⁻, the optimized R_{Pd-Cl} distance is longer than that of [PdCl₄]²⁻. In *cis*-PdCl₂Z₂, the \angle Cl-Pd-Cl and \angle Z-Pd-Z angles are wider than the angle of $\varphi = 90$ degrees.

In the dianionic *cis*-[PdZ₂(oxalate)] complexes with (Z = Cl⁻ and OH⁻), the optimized R_{Pd-O} distances between Pd and two binding O atoms of oxalate are longer than that of *cis*-[PdCl₂(OH)₂]²⁻ with the monodentate. On the other hand, in neutral *cis*-[PdZ₂(oxalate)] with (Z = OH₂, NH₃, PH₃), R_{Pd-O} between Pd and the O atoms is shorter. The optimized R_{Pd-Z} distances between Pd and (Z = Cl⁻, OH⁻, OH₂, NH₃, PH₃) in [PdZ₂(oxalate)] are longer than those of *cis*-[PdCl₂Z₂] with the corresponding monodentates. In *cis*-[PdZ₂(oxalate)], the internuclear distance (R_(Pd...C)^u \approx 2.8 Å) between the Pd atom and the ethylene group is shorter than that (R_(Pd...C)^u \approx 3.134 Å) of twisted *cis*-[Pd(PH₃)₂(oxalate)]. Due to the short internuclear distance of (R_(Pd...C)^u), the twisted *cis*-[PdZ₂(oxalate)] complexes are not optimized except for twisted *cis*-[Pd(PH₃)₂(oxalate)] with the tetrahedral geometry. The (\angle O-Pd-O) angles formed by the oxalate are narrower than $\varphi = 90$ degrees. The R_{Pd-O} and R_{Pd-PH₃} distances of *cis*-[Pd(PH₃)₂(oxalate)] are shorter and longer than those of twisted *cis*-[Pd(PH₃)₂(oxalate)], respectively.

With the relatively long R_(Pd...C)^v distance, the *cis*- and twisted *cis*-types of [PdZ₂(succinate)] with the 7-membered ring are optimized to be stable. The R_{Pd-O} and R_(Pd...C)^v distances of *cis*-[PdZ₂(succinate)] are longer those of the corresponding *cis*-[PdZ₂(oxalate)] complexes, respectively.

In [PdZ₂(succinate)] (Z = Cl⁻, OH⁻), the R_{Pd-O} distance in *cis*-isomer are relatively longer than those of twisted *cis*-isomer. On the other hand, in [PdZ₂(succinate)] (Z = NH₃, H₂O, PH₃), the R_{Pd-O} distance in *cis*-isomer are relatively shorter than those of twisted *cis*-isomer. In particular, in twisted *cis*-[PdZ₂(succinate)], the (R_(Pd...C)^v \approx 2.75 Å) distances between Pd(II) and the ethylene group are shorter than those (R_(Pd...C)^u \approx 2.8 Å) of *cis*-[Pd(Z)₂(oxalate)]. The distance between two orbitals is shorter than the sum of the van der Waals radii of the atoms concerned. That is, weak repulsion exists between two orbitals. As a result, the Pd(II) atom lies above the plane at a perpendicular distance of 1.0 and the four ligands are largely located out of the square planar array. The angles of (\angle O-Pd-O) and (\angle Z-Pd-Z) in twisted *cis*-[PdZ₂(succinate)] are narrower than $\varphi \approx 150$ degrees. If the (π -d_{z²}) intra-molecular interaction between the π -orbital and the d_{z²}-orbital occur, the angles of (\angle O-Pd-O) in twisted *cis*-[PdZ₂(succinate)] may be $\varphi \approx 150$ degrees.

In previously reported theoretical results,^{5,12,16-24} the shortest and longest (Pd-Cl) distances of [PdCl₄]²⁻ were 2.07 and 2.43 Å, respectively. Results from the Burda group¹⁹ suggest that the R_{Pd-Cl} distance varies from 2.2 Å in the neutral [PdCl₂Z₂] complex to 2.4 Å in the anionic [PdCl₂(OH)₂]²⁻ complex. According to the study of Pavankumar *et al.*,⁶ the metal-ligand distances (R_{M-Cl}, R_{M-Z}) are sensitive to the level of electron correlation and the size of the basis sets. In the previous experimental results,^{11,25-31} the shortest and longest (Pd-Cl) distances of [PdCl₄]²⁻ were 2.292 and 2.318 Å, respectively. In the study of Caminiti *et al.*,¹¹ the R_{Pd-Cl} distance in the first coordination shell (square-planar [PdCl₄]²⁻ units) was 2.02 Å, while the Pd-O distance of the Pd-OH₂ interactions bonded to the apical position was 2.315 Å.

The average atomic charges of the natural bond orbital analysis in Pd complexes are listed in Table 2. Our calculated charges are similar to the previously reported theoretical results.¹⁹ The absolute values of the atomic charges calculated at the B3P86/lan12dz levels are smaller than the corresponding values at any other level. In the Pd complexes, the charge values of the Pd(II) and P atoms are positive, whereas those of the other atoms are negative. Depending on the Z ligand, the atomic charges of Pd(II) are different from each other. That is, the atomic charges of Pd(II) coordinated with OH⁻ and PH₃ are the largest and smallest, respectively. The atomic charges of Pd(II) combined with the bidentate are more positive than those of Pd(II) with the monodentate. The atomic charge of Pd(II) in the *trans*- (twisted *cis*-) type is more positive than that in the *cis*-type. Meanwhile, in the Pd complexes combined with the P atom (σ -donor and π -acceptor) of PH₃, the redistribution of the atomic charge from Pd(II) to P-atom occurs *via* the π -acceptor of the empty d-orbital in the P atom. Therefore, the value of the atomic charge for P is relatively small.

In [PdCl₃Z]²⁻ with the anionic ligand, the atomic charges of *trans*-Cl are more negative, while, in [PdCl₃Z]⁻ with the neutral ligand, the atomic charges of *cis*-Cl are more negative. Because the atomic charges of the negatively charged OH⁻

Table 1. Optimized bond distances (Å) and angles (degree) of the equilibrium geometrical structures of [PdCl₃Z], [PdCl₂Z₂], [PdZ₂X], and [PdZ₂Y] at the some methods/6-311+G** (3-21G** for Pd) basis sets. R^c: atom of *cis*-position, R^t: atom of *trans*-position. The angle between two atoms in [PdCl₄]²⁻, [PdCl₃Br]²⁻, *cis*-[PdCl₂Br₂]²⁻, and [PdCl₂Z₂] is 90 degrees

compound	parameter	MP2	B1LYP	B3LYP	B3P86	B3P86 ^v	DFT	Exptl
[PdCl ₄] ²⁻	R _{Pd-Cl}	2.411	2.448	2.446	2.410	2.411	2.070 ^a , 2.30 ^{b,c} , 2.326 ^d , 2.39(2.43) ^e , 2.31(2.34) ^e , 2.154(2.192) ^f , 2.34(2.36) ^g , 2.360 ^h , 2.329(2.307) ⁱ , 2.350(2.402) ^j , 2.351(2.366) ^k	2.307 ^l , 2.318 ^m , 2.292 ⁿ , 2.309 ^o , 2.315 ^p , 2.30 ^q , 2.313 ^r , 2.302 ^s
[PdCl ₃ Br] ²⁻	R _{Pd-Br}	2.545	2.575	2.571	2.530	2.536		
	R _{Pd-Cl} ^c	2.407	2.445	2.443	2.407	2.410		
	R _{Pd-Cl} ^t	2.411	2.453	2.451	2.415	2.414		
[PdCl ₃ (OH)] ²⁻	R _{Pd-OH}	2.015	2.027	2.030	2.013	2.001	1.959 ^d	
	R _{Pd-Cl} ^c	2.459	2.495	2.491	2.449	2.455	2.389 ^d	
	R _{Pd-Cl} ^t	2.487	2.506	2.502	2.462	2.466	2.366, 2.332 ^d	
	∠Cl-Pd-Cl	93.5	92.9	92.9	92.8	93.2		
	∠Cl-Pd-O	87.0	87.1	87.1	87.2	86.9		
[PdCl ₃ (H ₂ O)] ⁻	R _{Pd-OH₂}	2.218	2.199	2.216	2.187	2.111	2.121 ^d	
	R _{Pd-Cl} ^c	2.380	2.408	2.409	2.377	2.381	2.297 ^d	
	R _{Pd-Cl} ^t	2.297	2.330	2.329	2.301	2.314	2.235 ^d	
	∠Cl-Pd-Cl	94.5	95.9	95.2	95.5	96.7		
	∠Cl-Pd-O	85.5	84.1	84.8	83.7	83.3		
[PdCl ₃ (NH ₃)] ⁻	R _{Pd-NH₃}	2.126	2.128	2.124	2.095	2.078		
	R _{Pd-Cl} ^c	2.385	2.421	2.419	2.386	2.406		
	R _{Pd-Cl} ^t	2.328	2.360	2.359	2.332	2.350		
	∠Cl-Pd-Cl	95.0	95.4	95.4	95.3	95.9		
[PdCl ₃ (PH ₃)] ⁻	R _{Pd-PH₃}	2.298	2.317	2.306	2.268	2.306		
	R _{Pd-Cl} ^c	2.380	2.415	2.414	2.382	2.399		
	R _{Pd-Cl} ^t	2.363	2.389	2.389	2.363	2.366		
	∠Cl-Pd-Cl	94.2	94.1	94.0	94.2	93.9		
<i>cis</i> -[PdCl ₂ Br ₂] ²⁻	R _{Pd-Cl}	2.408	2.442	2.442	2.407	2.413		
	R _{Pd-Br}	2.539	2.575	2.569	2.528	2.527		
<i>trans</i> -[PdCl ₂ Br ₂] ²⁻	R _{Pd-Cl}	2.403	2.440	2.440	2.405	2.405		
	R _{Pd-Br}	2.546	2.583	2.578	2.536	2.542		
<i>cis</i> -[PdCl ₂ (OH) ₂] ²⁻	R _{Pd-Cl}	2.536	2.568	2.564	2.514	2.514	2.407 ^d	
	R _{Pd-O}	2.046	2.055	2.057	2.043	2.020	1.973 ^d	
	∠Cl-Pd-Cl	97.8	97.7	97.8	97.6	99.2		
	∠O-Pd-O	88.2	89.5	89.6	89.9	90.5		
<i>trans</i> -[PdCl ₂ (OH) ₂] ²⁻	R _{Pd-Cl}	2.496	2.547	2.541	2.491	2.499	2.360 ^d	
	R _{Pd-O}	2.058	2.063	2.066	2.048	2.034	2.001 ^d	
<i>cis</i> -[PdCl ₂ (H ₂ O) ₂]	R _{Pd-Cl}	2.281	2.311	2.311	2.287	2.311	2.223 ^d	
	R _{Pd-O}	2.217	2.207	2.205	2.174	2.120	2.115 ^d	
	∠Cl-Pd-Cl	93.5	95.6	95.7	95.8	97.7		
	∠O-Pd-O	96.8	97.4	97.8	98.9	97.9		
<i>trans</i> -[PdCl ₂ (H ₂ O) ₂]	R _{Pd-Cl}	2.326	2.353	2.352	2.326	2.329	2.267 ^d	
	R _{Pd-O}	2.118	2.121	2.120	2.094	2.018	2.032 ^d	
<i>cis</i> -[PdCl ₂ (NH ₃) ₂]	R _{Pd-Cl}	2.310	2.343	2.343	2.318	2.320	2.254 ^d	
	R _{Pd-N}	2.167	2.169	2.165	2.134	2.101	2.070 ^d	
	∠Cl-Pd-Cl	94.1	95.2	95.2	95.2	96.1		
	∠N-Pd-N	97.2	97.4	97.6	97.7	98.5		
<i>trans</i> -[PdCl ₂ (NH ₃) ₂]	R _{Pd-Cl}	2.343	2.374	2.372	2.344	2.358	2.276 ^d	
	R _{Pd-N}	2.088	2.099	2.096	2.071	2.049	2.025 ^d	
<i>cis</i> -[PdCl ₂ (PH ₃) ₂]	R _{Pd-Cl}	2.358	2.385	2.385	2.362	2.371		
	R _{Pd-P}	2.311	2.340	2.332	2.294	2.303		
	∠Cl-Pd-Cl	96.6	96.4	96.4	97.3	95.1		
	∠P-Pd-P	102.9	103.1	103.1	104.0	102.5		
<i>trans</i> -[PdCl ₂ (PH ₃) ₂]	R _{Pd-Cl}	2.344	2.374	2.374	2.346	2.358		
	R _{Pd-P}	2.352	2.368	2.362	2.330	2.343		

Table 1. Continued

compound	parameter	MP2	B1LYP	B3LYP	B3P86	B3P86 ^v	DFT	Exptl
<i>cis</i> -[Pd(Cl) ₂ X] ²⁻	R _{Pd-Cl}	2.411	2.433	2.432	2.409	2.405		
	R _{Pd-O}	2.063	2.081	2.082	2.062	2.052		
	R _{Pd...C^f}	2.850	2.878	2.879	2.853	2.866		
	∠Cl-Pd-Cl	93.3	92.9	92.8	92.4	92.4		
	∠O-Pd-O	81.3	79.7	79.8	80.3	80.9		
<i>cis</i> -[Pd(OH) ₂ X] ²⁻	R _{Pd-OH}	2.054	2.067	2.069	2.049	2.016		
	R _{Pd-O}	2.111	2.118	2.117	2.094	2.081		
	R _{Pd...C^f}	2.889	2.907	2.906	2.877	2.883		
	∠HO-Pd-OH	91.5	92.5	92.5	92.5	92.5		
	∠O-Pd-O	80.2	79.1	79.2	79.8	80.7		
<i>cis</i> -[Pd(H ₂ O) ₂ X]	R _{Pd-OH₂}	2.221	2.218	2.219	2.190	2.177		
	R _{Pd-O}	1.972	1.991	1.995	1.978	1.964		
	R _{Pd...C^f}	2.772	2.790	2.792	2.768	2.793		
	∠H ₂ O-Pd-OH ₂	103.6	103.6	103.6	104.3	103.5		
	∠O-Pd-O	85.9	84.6	84.5	85.1	85.8		
<i>cis</i> -[Pd(NH ₃) ₂ X]	R _{Pd-NH₃}	2.171	2.177	2.176	2.145	2.130		
	R _{Pd-O}	1.987	2.008	2.011	1.995	1.984		
	R _{Pd...C^f}	2.777	2.801	2.803	2.779	2.805		
	∠N-Pd-N	104.3	104.7	104.8	105.0	105.9		
	∠O-Pd-O	85.8	84.2	84.2	84.7	85.4		
<i>cis</i> -[Pd(PH ₃) ₂ X]	R _{Pd-PH₃}	2.350	2.382	2.374	2.334	2.361		
	R _{Pd-O}	2.013	2.035	2.040	2.025	2.011		
	R _{Pd...C^f}	2.794	2.825	2.829	2.805	2.829		
	∠P-Pd-P	104.8	104.3	104.2	104.1	103.4		
	∠O-Pd-O	85.3	83.2	83.1	83.6	84.1		
twisted <i>cis</i> - [Pd(PH ₃) ₂ X]	R _{Pd-PH₃}	2.287	2.306	2.301	2.267	2.289		
	R _{Pd-O}	2.311	2.378	2.366	2.328	2.317		
	R _{Pd...C^f}	3.104	3.191	3.179	3.134	3.134		
	∠P-Pd-P	103.2	112.0	110.6	108.7	103.4		
	∠O-Pd-O	72.4	70.1	70.6	71.5	72.7		
<i>cis</i> -[Pd(Cl) ₂ Y] ²⁻	R _{Pd-Cl}	2.374	2.419	2.419	2.386	2.392		
	R _{Pd-O}	2.089	2.097	2.098	2.078	2.074		
	R _{Pd...C^u}	3.018	3.176	3.168	3.106	3.218		
	∠Cl-Pd-Cl	93.0	91.9	91.8	91.7	91.7		
	∠O-Pd-O	86.5	87.0	87.0	87.0	87.7		
twisted <i>cis</i> - [Pd(Cl) ₂ Y] ²⁻	R _{Pd-Cl}	2.390	2.434	2.435	2.400	2.409		
	R _{Pd-O}	2.071	2.099	2.101	2.071	2.065		
	R _{Pd...C^u}	2.770	2.854	2.856	2.785	2.827		
	∠Cl-Pd-Cl	173.3	167.0	167.4	170.0	171.4		
	∠O-Pd-O	148.2	142.7	142.6	146.3	146.9		
<i>cis</i> -[Pd(OH) ₂ Y] ²⁻	R _{Pd-OH}	2.039	2.052	2.054	2.035	2.025		
	R _{Pd-O}	2.140	2.140	2.128	2.116	2.090		
	R _{Pd...C^u}	3.206	3.340	3.334	3.275	3.308		
	∠OH-Pd-OH	91.0	91.9	91.9	92.2	92.4		
	∠O-Pd-O	90.7	91.7	91.9	92.2	94.7		
twisted <i>cis</i> - [Pd(OH) ₂ Y] ²⁻	R _{Pd-OH}	2.048	2.057	2.056	2.035	2.038		
	R _{Pd-O}	2.106	2.113	2.111	2.087	2.132		
	R _{Pd...C^u}	2.801	2.834	2.832	2.797	3.069		
	∠OH-Pd-OH	176.9	178.8	178.5	177.5	173.6		
	∠O-Pd-O	146.3	144.2	145.9	146.1	133.0		
<i>cis</i> -[Pd(H ₂ O) ₂ Y]	R _{Pd-OH₂}	2.200	2.201	2.202	2.173	2.161		
	R _{Pd-O}	1.980	1.991	1.994	1.978	1.955		
	R _{Pd...C^u}	3.136	3.377	3.378	3.323	3.479		
	∠H ₂ O-Pd-H ₂ O	102.9	103.5	103.7	104.4	104.5		
	∠O-Pd-O	95.5	99.8	99.9	99.8	106.1		

Table 1. Continued

compound	parameter	MP2	B1LYP	B3LYP	B3P86	B3P86 ^v	DFT	Exptl
twisted <i>cis</i> - [Pd(H ₂ O) ₂ Y]	R _{Pd-OH₂}	2.133	2.172	2.168	2.135	2.081		
	R _{Pd-O}	2.025	2.034	2.038	2.022	2.015		
	R _{Pd...C^u}	2.710	2.721	2.709	2.701	2.844		
	∠H ₂ O-Pd-H ₂ O	178.8	177.7	177.6	179.2	178.1		
	∠O-Pd-O	152.0	151.1	148.3	151.3	149.0		
<i>cis</i> -[Pd(NH ₃) ₂ Y]	R _{Pd-N}	2.152	2.163	2.162	2.132	2.106		
	R _{Pd-O}	2.003	2.016	2.018	2.003	1.980		
	R _{Pd...C^u}	3.123	3.348	3.346	3.276	3.326		
	∠N-Pd-N	101.9	101.9	102.1	102.4	101.8		
	∠O-Pd-O	94.5	97.4	97.3	97.0	103.7		
twisted <i>cis</i> - [Pd(NH ₃) ₂ Y]	R _{Pd-N}	2.093	2.144	2.141	2.090	2.057		
	R _{Pd-O}	2.108	2.159	2.156	2.104	2.034		
	R _{Pd...C^u}	2.709	2.720	2.719	2.707	2.785		
	∠N-Pd-N	175.9	176.7	176.1	176.4	179.5		
	∠O-Pd-O	149.0	147.4	147.7	148.4	146.3		
<i>cis</i> -[Pd(PH ₃) ₂ Y]	R _{Pd-P}	2.316	2.364	2.357	2.316	2.337		
	R _{Pd-O}	2.045	2.048	2.052	2.040	2.031		
	R _{Pd...C^u}	2.962	3.229	3.221	3.124	3.189		
	∠P-Pd-P	108.8	107.1	107.0	107.8	104.6		
	∠O-Pd-O	93.3	94.6	94.2	94.2	96.5		
twisted <i>cis</i> - [Pd(PH ₃) ₂ Y]	R _{Pd-P}	2.354	2.395	2.389	2.353	2.378		
	R _{Pd-O}	2.059	2.069	2.074	2.057	2.066		
	R _{Pd...C^u}	2.781	2.816	2.817	2.782	2.838		
	∠P-Pd-P	177.7	175.1	174.9	178.7	174.5		
	∠O-Pd-O	149.2	146.3	145.7	146.5	149.8		

^aRef. 16. ^bRef. 17. ^cRef. 18. ^dRef. 19. ^eRef. 5. ^fRef. 20. ^gRef. 21. ^hRef. 22. ⁱRef. 12. ^jRef. 23. ^kRef. 24. ^lRef. 25. ^mRef. 26. ⁿRef. 27. ^oRef. 28. ^pRef. 11. ^qRef. 29. ^rRef. 30. ^sRef. 31. ^uBond length between the carbon atom of the ethylene group in oxalate and the Pd atom. ^vBond length between the carbon atom of the ethylene group in succinate and the Pd atom. ^vValues were obtained at the B3P86/6-311+G** (lan12dz for Pd) level.

ligand move to the *trans*-Cl⁻ group via the central Pd atom, the atomic charges of *trans*-Cl are more negative. In [PdCl₂Z₂]²⁻ with the anionic ligand, the atomic charges of Cl in *cis*-type are also more negative than those of Cl in *trans*-type. Therefore, in [PdCl₃Z]²⁻ and [PdCl₂Z₂]²⁻ with the anionic ligand, these variations of the atomic charges are in good agreement with the variation of the bond distances. In *cis*-[PdZ₂(oxalate)], the atomic charges of the Pd(II) atom and the carbon atom of ethylene group are largely positive. In particular, due to the four negative oxygen atoms of oxalate, the atomic charges of the C atom in the ethylene group are largely positive (0.67 au). Therefore, due to the positive electrostatic repulsions between Pd(II) and the ethylene group, the twisted *cis*-[PdZ₂(oxalate)] complexes is not optimized. Meanwhile, in [PdZ₂(succinate)], the atomic charges of the Pd(II) center and the C atom in ethylene group of succinate have positive and small negative values, respectively. The atomic charges of the Pd(II) atom and the C atom in the twisted *cis*-type are more positive and negative than those of the *cis*-type, respectively. If the (π -d_{z²}) intramolecular interaction between the π -orbital and the d_{z²}-orbital occur, the atomic charges of the Pd(II) atom and the C atom in the twisted *cis*-type are less positive and negative than those of the *cis*-type, respectively.

The relative energies between the *cis*- and *trans*- (twisted

cis-) types in Pd complexes {[PdCl₂Z₂], (Z=Br⁻, OH⁻, H₂O, NH₃, PH₃) and [PdZ₂Y₂], (Z = Cl⁻, H₂O, NH₃, PH₃; Y = succinate)} are listed in Table 3. In [PdCl₂Z₂] with the monodentate, the relative energies are small and the *trans*-conformers are more stable than *cis*-conformers. While, in [PdZ₂Y₂] with the bidentate, the relative energies are relatively large and the twisted *cis*-types are much more unstable than the *cis*-types. That is, by an axial (d_{z²}- π) intramolecular repulsion between Pd(II) and the ethylene group, the structures of twisted *cis*-[PdZ₂(succinate)] are more unstable than those of the *cis*-[PdZ₂(succinate)]. The relative energies determined at the B3P86/lan12dz level are in the range of 1.08 eV for [Pd(PH₃)₂Y] to 1.54 eV for [Pd(NH₃)₂Y]. The relative energies in ([PdCl₂Z₂] and [PdZ₂Y₂]) complexes with Z = NH₃ are largest. Our energy difference between the *cis*- and twisted *cis*-[PdZ₂Y₂] complexes calculated at the B3P86/lan12dz level is about 1.3 eV. The (d_{z²}- π) repulsion between the two orbitals plays an important role in the relative stability. The relative energies in [PdZ₂Y₂] complexes with Z = PH₃ are smallest. These small energy gaps could be a consequence of enhanced π -back donation of the atomic charges from the Pd(II) center to the P atom. The charge balance of the ligand coordinated to the central Pd(II) atom influences the geometrical configuration and the bond length between Pd(II) and the ligands. In particular, the electronic

Table 2. Average atomic charges (au, NBO) of the equilibrium structures of [PdCl₃Z], [PdCl₂Z₂], [PdZ₂X], and [PdZ₂Y] at the various methods/6-311+G** (3-21G** for Pd) basis set. Q^c = charge of *cis*-position, Q^t = charge of *trans*-position

compound	charge	MP2	B1LYP	B3LYP	B3p86	B3p86 ^h	MP2
[PdCl ₄] ²⁻	Q _{Pd}	1.146	0.846	0.823	0.791	0.560	0.537 ^g
	Q _{Cl}	-0.787	-0.712	-0.706	-0.698	-0.640	-0.631 ^g
[PdCl ₃ Br] ²⁻	Q _{Pd}	1.119	0.821	0.799	0.766	0.532	
	Q ^c _{Cl}	-0.780	-0.708	-0.703	-0.694	-0.633	
	Q ^t _{Cl}	-0.783	-0.711	-0.706	-0.698	-0.636	
	Q _{Br}	-0.775	-0.695	-0.688	-0.680	-0.631	
[PdCl ₃ OH] ²⁻	Q _{Pd}	1.224	0.912	0.888	0.857	0.648	0.657 ^g
	Q ^c _{Cl}	-0.839	-0.771	-0.765	-0.755	-0.687	-0.665 ^g
	Q ^t _{Cl}	-0.853	-0.790	-0.784	-0.774	-0.713	-0.712 ^g
	Q _O	-1.121	-1.004	-0.999	-0.998	-0.997	-1.033 ^g
[PdCl ₃ (H ₂ O)] ⁻	Q _{Pd}	1.125	0.835	0.810	0.780	0.637	0.571 ^g
	Q ^c _{Cl}	-0.760	-0.682	-0.667	-0.657	-0.607	-0.609 ^g
	Q ^t _{Cl}	-0.655	-0.556	-0.547	-0.541	-0.515	-0.466 ^g
	Q _O	-0.947	-0.902	-0.909	-0.908	-0.951	-0.949 ^g
[PdCl ₃ (NH ₃)] ⁻	Q _{Pd}	1.109	0.818	0.795	0.767	0.593	
	Q ^c _{Cl}	-0.772	-0.690	-0.684	-0.675	-0.615	
	Q ^t _{Cl}	-0.707	-0.613	-0.608	-0.603	-0.564	
	Q _N	-1.018	-0.988	-0.986	-0.991	-1.073	
[PdCl ₃ PH ₃] ⁻	Q _{Pd}	0.948	0.720	0.701	0.672	0.470	
	Q ^c _{Cl}	-0.729	-0.643	-0.635	-0.625	-0.571	
	Q ^t _{Cl}	-0.729	-0.628	-0.623	-0.623	-0.554	
	Q _P	0.336	0.213	0.204	0.185	0.171	
<i>cis</i> -[PdCl ₂ Br ₂] ²⁻	Q _{Pd}	1.090	0.795	0.773	0.739	0.502	
	Q _{Cl}	-0.777	-0.705	-0.701	-0.693	-0.628	
	Q _{Br}	-0.768	-0.692	-0.686	-0.677	-0.623	
<i>trans</i> -[PdCl ₂ Br ₂] ²⁻	Q _{Pd}	1.091	0.797	0.775	0.741	0.504	
	Q _{Cl}	-0.774	-0.704	-0.699	-0.691	-0.626	
	Q _{Br}	-0.771	-0.694	-0.688	-0.680	-0.626	
<i>cis</i> -[PdCl ₂ (OH) ₂] ²⁻	Q _{Pd}	1.265	0.948	0.917	0.895	0.688	0.738 ^g
	Q _{Cl}	-0.887	-0.835	-0.838	-0.817	-0.753	-0.736 ^g
							-0.766
	Q _O	-1.160	-1.068	-1.039	-1.061	-1.024	-1.129 ^g
<i>trans</i> -[PdCl ₂ (OH) ₂] ²⁻	Q _{Pd}	1.307	0.986	0.961	0.929	0.722	0.758 ^g
	Q _{Cl}	-0.873	-0.822	-0.815	-0.803	-0.725	-0.720 ^g
	Q _O	-1.200	-1.090	-1.084	-1.081	-1.066	-1.119 ^g
<i>cis</i> -[PdCl ₂ (H ₂ O) ₂]	Q _{Pd}	1.129	0.849	0.829	0.806	0.721	0.620 ^g
	Q _{Cl}	-0.624	-0.510	-0.503	-0.498	-0.472	-0.433 ^g
	Q _O	-0.956	-0.915	-0.912	-0.908	-0.959	-0.958 ^g
<i>trans</i> -[PdCl ₂ (H ₂ O) ₂]	Q _{Pd}	1.238	0.934	0.910	0.882	0.797	0.751 ^g
	Q _{Cl}	-0.716	-0.604	-0.597	-0.595	-0.563	-0.565 ^g
	Q _O	-0.929	-0.877	-0.872	-0.867	-0.945	-0.913 ^g
<i>cis</i> -[PdCl ₂ (NH ₃) ₂]	Q _{Pd}	1.090	0.806	0.783	0.764	0.628	0.537 ^g
	Q _{Cl}	-0.669	-0.565	-0.558	-0.554	-0.516	-0.484 ^g
	Q _N	-1.051	-1.012	-1.010	-1.018	-1.087	-1.094 ^g
<i>trans</i> -[PdCl ₂ (NH ₃) ₂]	Q _{Pd}	1.104	0.819	0.798	0.770	0.633	0.569 ^g
	Q _{Cl}	-0.736	-0.642	-0.636	-0.630	-0.578	-0.574 ^g
	Q _N	-1.002	-0.959	-0.958	-0.961	-1.051	-1.042 ^g
<i>cis</i> -[PdCl ₂ (PH ₃) ₂]	Q _{Pd}	0.769	0.604	0.591	0.559	0.374	
	Q _{Cl}	-0.658	-0.554	-0.547	-0.543	-0.482	
	Q _P	0.297	0.183	0.173	0.157	0.136	
<i>trans</i> -[PdCl ₂ (PH ₃) ₂]	Q _{Pd}	0.797	0.608	0.592	0.561	0.377	
	Q _{Cl}	-0.681	-0.588	-0.581	-0.573	-0.513	
	Q _P	0.307	0.207	0.197	0.173	0.162	

Table 2. Continued

compound	charge	MP2	B1LYP	B3LYP	B3p86	B3p86 ^h	MP2
<i>cis</i> -[PdCl ₂ X] ²⁻	Q _{Pd}	1.260	0.925	0.899	0.873	0.738	
	Q _{Cl}	-0.794	-0.724	-0.718	-0.708	-0.644	
	Q _O ^b	-0.889	-0.729	-0.716	-0.709	-0.729	
	Q _C ^c	0.837	0.683	0.671	0.664	0.693	
<i>cis</i> -[Pd(OH) ₂ X] ²⁻	Q _{Pd}	1.343	1.003	0.977	0.955	0.826	
	Q _{OH} ^a	-1.185	-1.083	-1.076	-1.072	-1.044	
	Q _O ^b	-0.922	-0.787	-0.776	-0.769	-0.779	
	Q _C ^c	0.841	0.685	0.673	0.666	0.695	
<i>cis</i> -[Pd(H ₂ O) ₂ X]	Q _{Pd}	1.314	0.969	0.945	0.927	0.902	
	Q _{OH₂} ^d	-0.960	-0.923	-0.921	-0.917	-0.969	
	Q _O ^b	-0.899	-0.711	-0.699	-0.696	-0.733	
	Q _C ^c	0.827	0.689	0.678	0.671	0.703	
<i>cis</i> -[Pd(NH ₃) ₂ X]	Q _{Pd}	1.249	0.913	0.889	0.870	0.801	
	Q _N	-1.055	-1.022	-1.022	-1.024	-1.092	
	Q _O ^b	-0.914	-0.738	-0.726	-0.723	-0.760	
	Q _C ^c	0.830	0.690	0.679	0.672	0.705	
<i>cis</i> -[Pd(PH ₃) ₂ X]	Q _{Pd}	0.963	0.731	0.713	0.688	0.580	
	Q _P	0.250	0.139	0.128	0.111	0.125	
	Q _O ^b	-0.909	-0.731	-0.719	-0.717	-0.739	
	Q _C ^c	0.825	0.689	0.678	0.670	0.704	
twisted <i>cis</i> -[Pd(PH ₃) ₂ X]	Q _{Pd}	0.451	0.436	0.449	0.443	0.274	
	Q _P	0.148	0.095	0.054	0.078	0.007	
	Q _O ^b	-0.939	-0.842	-0.834	-0.828	-0.832	
	Q _C ^c	0.840	0.677	0.665	0.660	0.690	
<i>cis</i> -[PdCl ₂ Y] ²⁻	Q _{Pd}	1.255	0.934	0.909	0.883	0.754	
	Q _{Cl}	-0.776	-0.698	-0.692	-0.684	-0.632	
	Q _O ^e	-0.863	-0.708	-0.696	-0.688	-0.716	
	Q _C ^f	-0.265	-0.273	-0.274	-0.282	-0.301	
twisted <i>cis</i> -[PdCl ₂ Y] ²⁻	Q _{Pd}	1.262	0.950	0.926	0.896	0.779	
	Q _{Cl}	-0.785	-0.705	-0.700	-0.695	-0.643	
	Q _O ^e	-0.865	-0.712	-0.700	-0.688	-0.712	
	Q _C ^f	-0.269	-0.278	-0.279	-0.286	-0.305	
<i>cis</i> -[Pd(OH) ₂ Y] ²⁻	Q _{Pd}	1.341	1.013	0.898	0.967	0.840	
	Q _{OH} ^a	-1.172	-1.059	-1.052	-1.049	-1.030	
	Q _O ^e	-0.895	-0.767	-0.757	-0.750	-0.766	
	Q _C ^f	-0.262	-0.273	-0.274	-0.282	-0.302	
twisted <i>cis</i> -[Pd(OH) ₂ Y] ²⁻	Q _{Pd}	1.359	1.059	1.056	1.043	0.932	
	Q _{OH} ^a	-1.196	-1.063	-1.057	-1.065	-1.064	
	Q _O ^e	-0.928	-0.780	-0.769	-0.764	-0.769	
	Q _C ^f	-0.262	-0.256	-0.257	-0.265	-0.280	
<i>cis</i> -[Pd(H ₂ O) ₂ Y]	Q _{Pd}	1.345	1.015	0.989	0.970	0.950	
	Q _{OH₂} ^b	-0.962	-0.918	-0.915	-0.911	-0.964	
	Q _O ^e	-0.898	-0.736	-0.724	-0.720	-0.777	
	Q _C ^f	-0.262	-0.256	-0.257	-0.265	-0.280	
twisted <i>cis</i> -[Pd(H ₂ O) ₂ Y]	Q _{Pd}	1.390	1.065	1.043	1.016	1.001	
	Q _{OH₂} ^b	-0.979	-0.900	-0.891	-0.889	-0.949	
	Q _O ^e	-0.866	-0.718	-0.710	-0.703	-0.749	
	Q _C ^f	-0.266	-0.302	-0.305	-0.310	-0.325	
<i>cis</i> -[Pd(NH ₃) ₂ Y]	Q _{Pd}	1.270	0.949	0.924	0.906	0.842	
	Q _N	-1.051	-1.013	-1.012	-1.015	-1.078	
	Q _O ^e	-0.904	-0.751	-0.738	-0.731	-0.799	
	Q _C ^f	-0.266	-0.262	-0.263	-0.272	-0.282	
twisted <i>cis</i> -[Pd(NH ₃) ₂ Y]	Q _{Pd}	1.370	1.016	1.008	0.992	0.949	
	Q _N	-1.036	-1.005	-1.002	-0.997	-1.056	
	Q _O ^e	-0.913	-0.777	-0.730	-0.733	-0.757	
	Q _C ^f	-0.285	-0.303	-0.306	-0.312	-0.330	
<i>cis</i> -[Pd(PH ₃) ₂ Y]	Q _{Pd}	0.950	0.743	0.724	0.696	0.598	
	Q _P	0.282	0.178	0.167	0.151	0.150	
	Q _O ^e	-0.892	-0.740	-0.726	-0.718	-0.757	
	Q _C ^f	-0.274	-0.268	-0.269	-0.281	-0.290	
twisted <i>cis</i> -[Pd(PH ₃) ₂ Y]	Q _{Pd}	0.966	0.755	0.737	0.714	0.607	
	Q _P	0.290	0.184	0.172	0.154	0.149	
	Q _O ^e	-0.876	-0.721	-0.709	-0.700	-0.720	
	Q _C ^f	-0.311	-0.303	-0.304	-0.315	-0.327	

^aAtomic charges of O in OH. ^bAtomic charges of the binding O atom in oxalate. ^cAtomic charges of the carbon atom in the ethylene group of oxalate. ^dAtomic charges of O in H₂O. ^eAtomic charges of the binding O atom in succinate. ^fAtomic charges of the carbon atom in the ethylene group of succinate. ^hRef. 19. ^hValues are calculated at the B3P86/6-311+G** (lan12dz for Pd) level.

Table 3. Relative energies (eV) between the *cis*- and *trans* (twisted *cis*)-types of the equilibrium PdCl₂Z₂ and PdZ₂Y (Y = CO₂⁻CHCHCO₂⁻) complexes at the various methods/6-311+G** (3-21G** for Pd) basis set

compound	type	MP2	B1LYP	B3LYP	B3p86	B3p86 ^a
[PdCl ₂ Br ₂] ²⁻	<i>cis</i>	0.00	0.00	0.00	0.00	0.00
	<i>trans</i>	-0.01	-0.01	-0.01	-0.00	-0.01
[PdCl ₂ (OH) ₂] ²⁻	<i>cis</i>	0.00	0.00	0.00	0.00	0.00
	<i>trans</i>	-0.03	-0.03	-0.02	-0.02	-0.02
[PdCl ₂ (H ₂ O) ₂]	<i>cis</i>	0.00	0.00	0.00	0.00	0.00
	<i>trans</i>	-0.02	-0.02	-0.02	-0.02	-0.02
[PdCl ₂ (NH ₃) ₂]	<i>cis</i>	0.00	0.00	0.00	0.00	0.00
	<i>trans</i>	-0.54	-0.56	-0.55	-0.53	-0.54
[PdCl ₂ (PH ₃) ₂]	<i>cis</i>	0.00	0.00	0.00	0.00	0.00
	<i>trans</i>	-0.30	-0.35	-0.34	-0.25	-0.31
[PdCl ₂ Y] ²⁻	<i>cis</i>	0.00	0.00	0.00	0.00	0.00
	twisted	1.37	1.33	1.31	1.27	1.29
	<i>cis</i>					
[Pd(OH) ₂ Y] ²⁻	<i>cis</i>	0.00	0.00	0.00	0.00	0.00
	twisted	1.33	1.38	1.35	1.32	1.32
	<i>cis</i>					
[Pd(H ₂ O) ₂ Y]	<i>cis</i>	0.00	0.00	0.00	0.00	0.00
	twisted	1.33	1.32	1.32	1.31	1.32
	<i>cis</i>					
[Pd(NH ₃) ₂ Y]	<i>cis</i>	0.00	0.00	0.00	0.00	0.00
	twisted	1.56	1.60	1.59	1.52	1.43
	<i>cis</i>					
[Pd(PH ₃) ₂ Y]	<i>cis</i>	0.00	0.00	0.00	0.00	0.00
	twisted	1.14	1.16	1.15	1.08	1.08
	<i>cis</i>					

^aValues were evaluated at the B3P86/6-311+G** (lanl2dz for Pd) level.

neutralization between the positively charged Pd(II) center and the negatively charged ligands contributes to the binding strengths and relative stabilities.

Potential energy curves for ligand exchange reactions.

To investigate the direct interaction between the central Pd(II) cation and the fifth ligand, the potential energy curves of the ligand exchange reactions from (PdZ₂Cl₂ + H₂O; Z = NH₃, PH₃) to (PdZ₂ClH₂O + Cl⁻) are calculated for R_{Pd-Cl} and R_{Pd-O}. The potential energy surface (a) and contour map (b) for the ligand exchange processes of ([PdZ₂Cl₂]···OH₂), **A** → {([PdZ₂Cl]⁺···[OH₂][Cl⁻]), **B**} → {([PdZ₂Cl(OH₂)]⁺···Cl⁻), **C**} are presented in Figures 2 and 4. To compare the reactivities in the ligand exchange reactions, we selected the NH₃ (hard σ-donor) and PH₃ (σ-donor and π-acceptor) ligands. In Figure 2, the internuclear distances range from 2.0 to 4.5 Å for (Pd-O) and from 2.3 to 4.25 Å for (Pd-Cl). **A** and **C** are stable states for both the reactant and product, and **B** is a transition state. **A** and **C** are not the positions of the asymptotes. At the **A** position, ([Pd(NH₃)₂Cl₂]···OH₂), with two hydrogen bond interactions (R_(Cl···H₂O) = 2.229 Å, R_(H₂NH···OH₂) = 1.764 Å) is optimized. That is, ([Pd(NH₃)₂Cl₂]···OH₂) with a 6-membered (Pd-OH···Cl···HN) interaction is optimized to the geometrical structure of a second water solvation shell. The five-coordinated Pd(II) complexes cannot be optimized with a vertical (Pd···OH₂)

interaction. The geometrical structure at the transition state of **B** is a pentacoordinated Pd complex with a direct (Pd···OH₂) interaction. The geometry is not a regular square pyramidal structure. The Pd(II) metal combines with an entering H₂O and a leaving Cl, and the entering H₂O simultaneously forms two hydrogen-bond with a leaving Cl⁻ and a hydrogen from NH₃. The distances of R_(Cl···H₂O) and R_(H₂NH···OH₂) at **B** are 2.165 and 2.193 Å, respectively. At point **C**, the stable structure with two hydrogen bond (R_(Cl···H₂O) = 1.864 Å, R_(Cl···HNH₂) = 2.082 Å) between H₂O and Cl⁻ and between NH₃ and Cl⁻ is optimized. (b) in Figure 2 shows only the potential energy surfaces produced by the projection for the 3-dimensional axis (x-R_(Pd-Cl), y-R_(Pd-O), z-energy axis) of (a). From the reactant ([Pd(NH₃)₂Cl₂]···OH₂) to the product ([Pd(NH₃)₂Cl(OH₂)]⁺···Cl⁻), the ligand exchange reactions take place through the transition state surface. The solid lines indicate the estimated potential valley surfaces and these are drawn by hand. The ligand exchange reactions are very slightly endothermic.

To clarify the mechanisms for the exchange reactions, the variations of the geometrical structures, relative potential energies, and HOMO/LUMO from (Pd(NH₃)₂Cl₂ + H₂O) to (Pd(NH₃)₂ClH₂O + Cl⁻) were investigated in detail using five sets of reaction. The results are presented in Figure 3. The potential energy of the **A** complex is set to zero. The HOMO and LUMO are represented as the top view. At position **A**, the d_{yz}-orbital of the central Pd atom is the HOMO and the d_{x²-y²} orbital is the LUMO. At position **D**, the water molecule is located on the upside of the [Pd(NH₃)₂Cl₂] complex. The relative energy of **D** with respect to **A** is 0.29 eV. At position **B**, Pd(II) with the pentacoordinated geometry simultaneously interacts with an entering H₂O and a leaving Cl. The water molecule is located on the upside of the [Pd(NH₃)₂Cl₂] complex. The angles of ∠Pd-N-O, ∠O-Pd-N, and ∠O-Pd-Cl are 59.0, 74.6, and 68.8 degrees, respectively. The (Pd-H₂O) interaction corresponds to neither ∠O-Pd-Cl = 90.0 degrees nor C_{2v}-symmetry. The small d_{z²}-orbital is the HOMO and the d_{x²-y²}-orbital is the LUMO. The relative energy of **B** with respect to **A** is 0.66 eV. At the **E** position, the departing Cl atom of the (Pd-Cl) bond is disconnecting from [Pd(NH₃)₂Cl₂]. The chloride is located on the downside of the [Pd(NH₃)₂Cl(H₂O)] complex. The relative energy of **C** with respect to **A** is 0.08 eV. The geometry of the product corresponds to a square planar structure. The departing Cl⁻ continuously interacts with the two hydrogen atoms of H₂O and NH₃.

In Figure 4, the internuclear distances range from 2.0 to 4.5 Å for (Pd-O) and from 2.2 to 4.25 Å for (Pd-Cl). **A** and **C** correspond to the equilibrium states of the reactant and product, respectively, and **B** is the point corresponding to the transition state. At position **A**, ([PdCl₂(PH₃)₂]···H₂O) with two hydrogen bonds of (Pd-OH···Cl···HP) is optimized. That is, the chloride and the hydrogen atom of PH₃ in [Pd(PH₃)₂Cl₂] interact with the hydrogen and oxygen atoms of H₂O, respectively. The ([PH₃)₂Cl₂Pd···OH₂] complex with the vertical (Pd···OH₂) interaction at the axial position cannot be optimized. The potential curve of **i** (R_{Pd-O} = 3.75

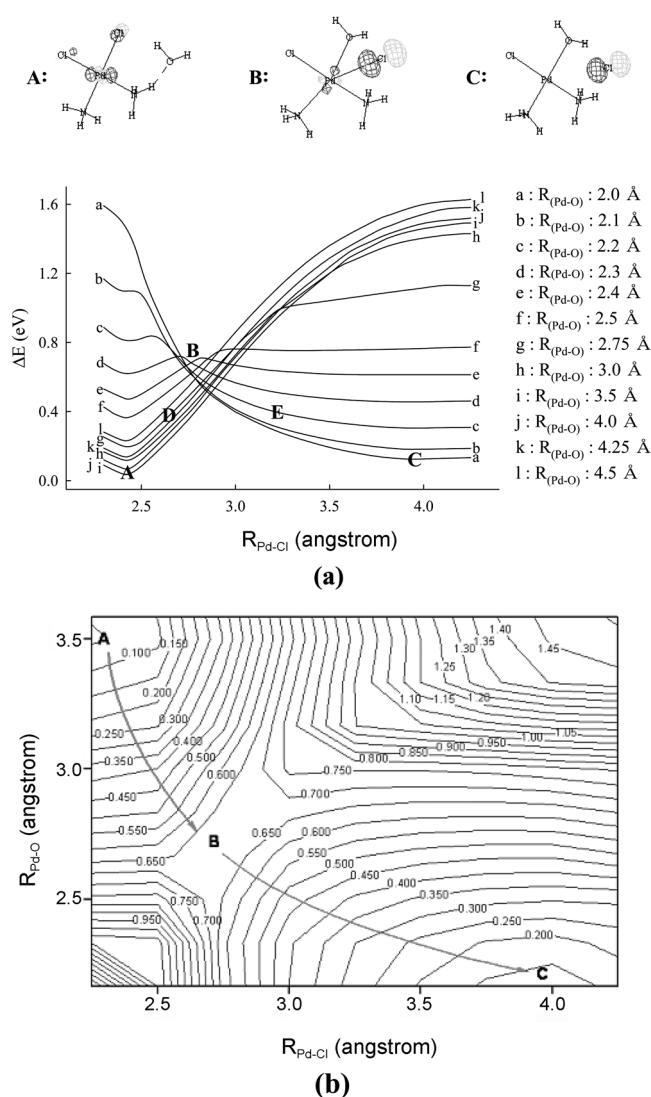


Figure 2. Potential energy surface (a) and corresponding contour map (b) for the ligand exchange processes involving the reactant $\{([Pd(NH_3)_2Cl_2] \cdots OH_2), \mathbf{A}\}$, the transition state $\{([Pd(NH_3)_2Cl] \cdots [OH_2][Cl^-]), \mathbf{B}\}$, and the product $\{([Pd(NH_3)_2Cl(OH_2)]^+ \cdots Cl^-), \mathbf{C}\}$ at the B3P86/6-311+G** (3-21G** for Pd) levels. All energies are adiabatic values and are in units of eV.

Å) has the lowest energy level around the **A** position. At the transition state of **B**, the geometrical structure for the ligand exchange processes is a pentacoordinated Pd complex with a square pyramidal geometry. The Pd(II) metal apically combines with an entering H_2O and a leaving Cl is located on the outer side of the square $[Pd(NH_3)_2Cl_2]$ frame. The Pd-Cl bond distance increases. At point **C**, the stable structure with the hydrogen bond ($R_{Cl \cdots H_2O} = 1.882 \text{ \AA}$, $R_{Cl \cdots HPH_2} = 2.057 \text{ \AA}$) between H_2O and Cl^- is optimized to a square planar geometry. Figure 4 (b) shows the projection of Figure 3 (a) for the 3-dimensional axis ($x-R_{Pd-Cl}$, $y-R_{Pd-O}$, z -energy axis). From $([Pd(PH_3)_2Cl_2] \cdots OH_2)$ to $([Pd(PH_3)_2Cl(OH_2)]^+ \cdots Cl^-)$, the direction of the reaction path is denoted by the solid lines on the contour map and the lines are drawn by hand.

The variations in the geometrical structures, relative

potential energies, and HOMO/LUMO from $(Pd(PH_3)_2Cl_2 + H_2O)$ to $(Pd(PH_3)_2ClH_2O + Cl^-)$ were investigated. The results are presented in Figure 5. At position **A**, the geometry of $([Pd(PH_3)_2Cl_2] \cdots H_2O)$ is not a planar structure. In $[Pd(PH_3)_2Cl_2] \cdots H_2O$, a 6-membered $(PdCl \cdots HO \cdots HP)$ interaction is formed by means of two hydrogen bonds. The size of the HOMO of the departing Cl atom is large. At position **D**, the water molecule is axially located on the square planar $[Pd(PH_3)_2Cl_2]$ complex. The relative energy of **D** with respect to **A** is 0.12 eV. At position **B**, the geometrical structure is one transition state corresponding to a square pyramidal $([Pd(PH_3)_2Cl][H_2O][Cl^-])^\ddagger$ complex. The (Pd-Cl) bond length increases and simultaneously the distance between Pd(II) and the oxygen atom in H_2O decreases. The fifth H_2O molecule is vertically located on the square planar $[Pd(PH_3)_2Cl_2]$ complex. That is, by the departure of Cl^- from $[Pd(PH_3)_2Cl_2]$, the space of the up and down sides of the Pd complexes is widened. And then the fifth H_2O ligand can axially approach the d_{z^2} -orbital of Pd [d -orbital of Pd(II) interacts with the lone pair orbital of H_2O at the axial direct, and the four ligands simultaneously interact with a $d_{x^2-y^2}$ orbital of Pd(II)]. Meanwhile, when the lone pair electron of the P atom (σ -donor and π -acceptor, Lewis base) in PH_3 bonds to the central Pd(II) (Lewis acid), the electronic density transfer from the occupied d_{xy} -orbital in Pd to the empty d-orbitals of the P atom occurs *via* π -acceptor back donation. Therefore, with the departure of Cl^- and the π -orbital back donation, the apical $(Pd \cdots H_2O)$ interaction at the axial position of the square planar $[Pd(PH_3)_2Cl_2]$ complexes occurs strongly. The angles of O-Pd-Cl and O-Pd-P are 87.1 and 92.9 degrees, respectively. The large d_{z^2} -orbital is the HOMO and the $d_{x^2-y^2}$ orbital is the LUMO. The relative energy of **B** with respect to **A** is 0.40 eV. At position **E**, the departing Cl^- is located on the downside of the square planar $[Pd(NH_3)_2Cl(H_2O)]$ complex. The (Pd-Cl) bond is disconnected and the structure of $([Pd(PH_3)_2Cl(H_2O)]^+)$ is rearranged to have a distorted square planar geometry. At position **C**, the departing Cl^- group is horizontally located in the middle of the H_2O and PH_3 molecules and connected with two hydrogen-bonds. The relative energy of **C** with respect to **A** is 0.20 eV. The p -orbital of the departing Cl^- is the HOMO and the $d_{x^2-y^2}$ orbital is the LUMO. The vertical $(Pd \cdots H_2O)$ interaction in $(Pd(PH_3)_2Cl_2)$ is stronger than that in $(Pd(NH_3)_2Cl_2)$. The relative energies for the ligand exchange reactions from $(Pd(PH_3)_2Cl_2 + H_2O)$ to $(Pd(PH_3)_2ClH_2O + Cl^-)$ are lower than those from $(Pd(NH_3)_2Cl_2 + H_2O)$ to $(Pd(NH_3)_2ClH_2O + Cl^-)$. Our results for the ligand exchange reactions are in line with the results of hydrolysis reactions for the Pt complexes investigated by Santos group.⁸

Conclusions

We investigated the geometrical structures of Pd(II) complexes and potential energy surfaces for the ligand exchange reactions of Pd(II) complexes in relation to their ligand-solvent interactions. In the optimized Pd complexes, Pd(II)

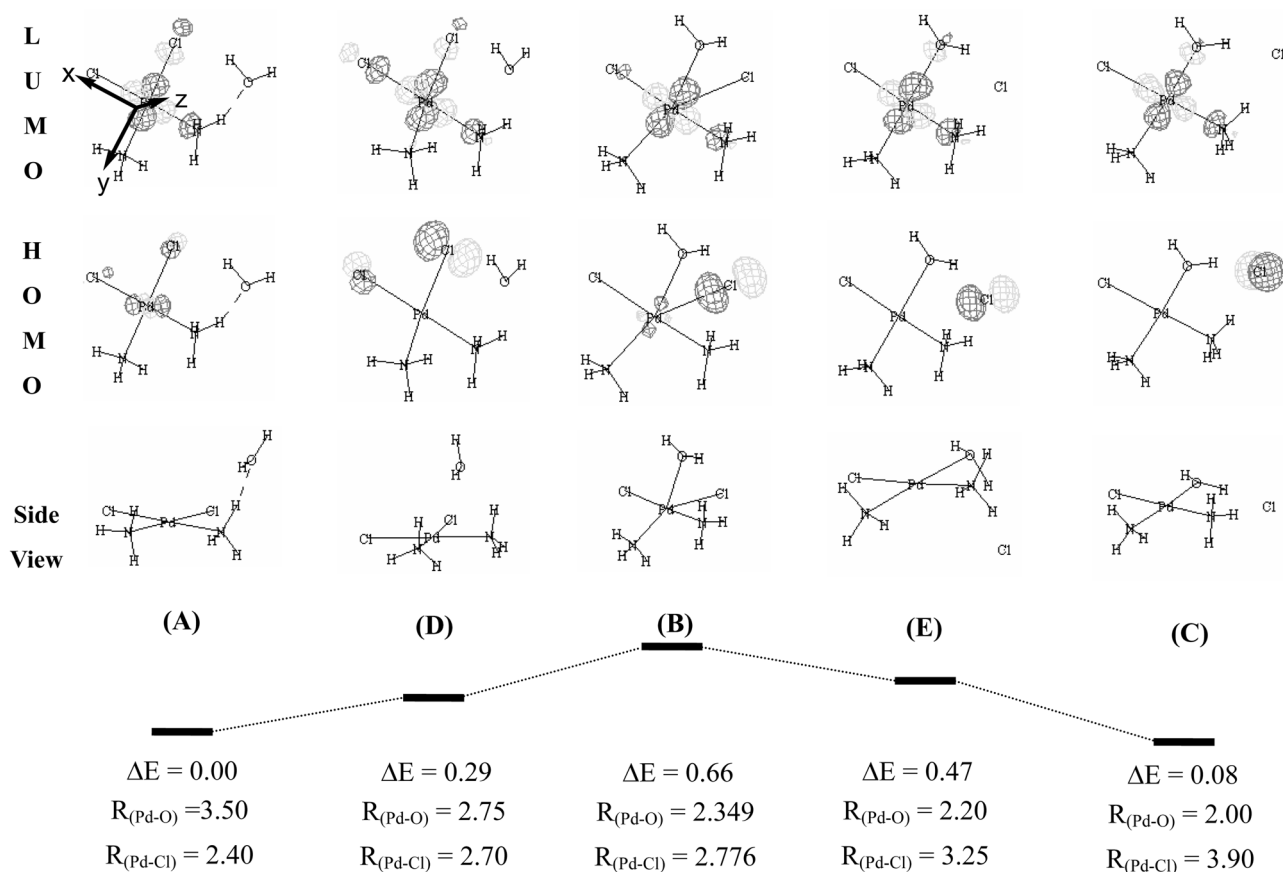


Figure 3. Geometrical structures and relative potential energies for the ligand exchange of $([PdCl_2(NH_3)_2] \cdots OH_2)$ into $([PdCl(NH_3)_2(OH_2)]^+ + Cl^-)$ including HOMO and LUMO at the B3P86/6-311+G** (3-21G** for Pd) levels. All energies are adiabatic values and are in units of eV. Bond lengths are in angstroms.

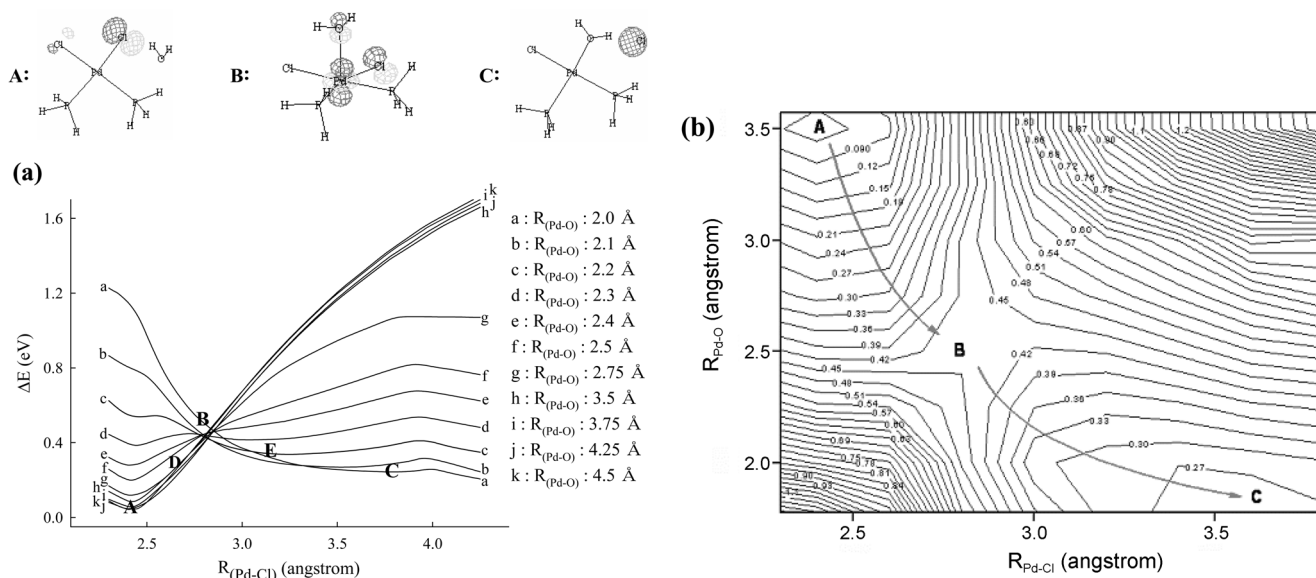


Figure 4. Potential energy surface (a) and corresponding contour map (b) for the ligand exchange processes covering the reactant $\{([PdCl_2(PH_3)_2] \cdots OH_2), \mathbf{A}\}$, the transition state $\{([PdCl(PH_3)_2]^+ \cdots [OH_2][Cl^-]), \mathbf{B}\}$, and the product $\{([PdCl(PH_3)_2(OH_2)]^+ \cdots Cl^-), \mathbf{C}\}$ at the B3P86/6-311+G** (3-21G** for Pd) levels. All energies are adiabatic values and are in unit of eV.

is located at the center of the distorted square planar structure surrounded by four neutral and anionic ligands. In $[PdCl_3Z]^{2-}$ with the anionic ligand, R_{Pd-Cl}^t of the *trans*-

position are longer than R_{Pd-Cl}^c of the *cis*-position. In $PdCl_2Z_2$, the structures of the *trans*-type are more stable than those of the *cis*-type. In $[PdZ_2(oxalate)]$ with bidentate, the

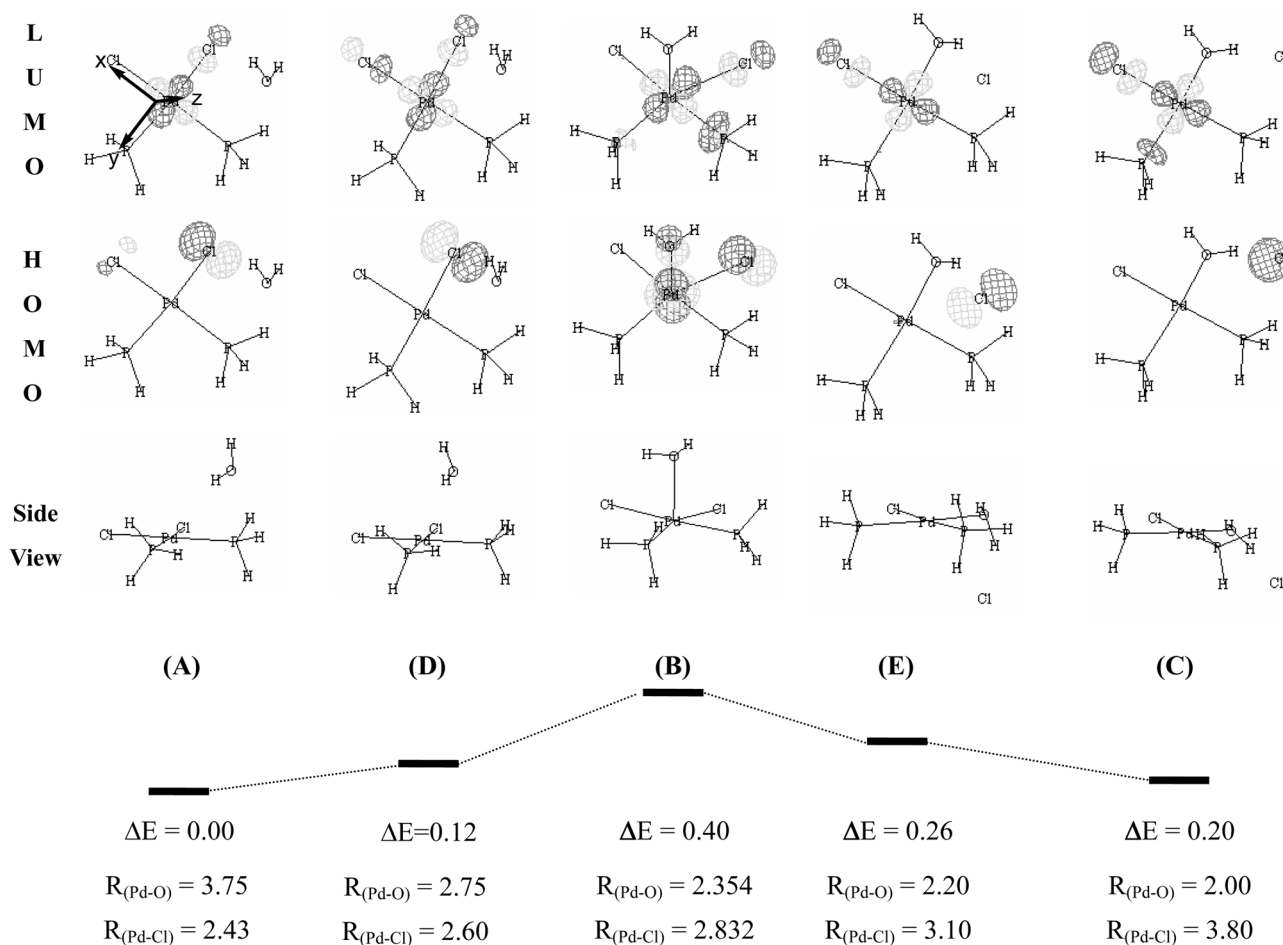


Figure 5. Schematic diagram for the ligand exchange of $([PdCl_2(PH_3)_2] \cdots OH_2)$ into $([PdCl(PH_3)_2(OH_2)]^+ \cdots Cl^-)$ including HOMO and LUMO at the B3P86/6-311+G** (3-21G** for Pd) levels. All energies are adiabatic values and are in units of eV. Bond lengths are in angstroms.

cis-type with a five membered-ring is only optimized except for twisted *cis*- $[Pd(PH_3)_2(\text{oxalate})]$. The twisted *cis*-types are not optimized due to the $(d_{z^2}-\pi)$ intra-molecular repulsion. In $[PdZ_2(\text{succinate})]$, the *cis*- and twisted *cis*-types with a seven membered-ring are optimized to be stable. In twisted *cis*- $[PdZ_2(\text{succinate})]$, the succinate ligand is located at the axial plane in parallel with the d_{z^2} -orbital. Due to the weakly $(\pi-d_{z^2})$ intra-molecular repulsion, the structures of twisted *cis*- $[PdZ_2(\text{succinate})]$ are not co-planar with the four donor atoms and the twisted *cis*-type are more unstable than the *cis*-type. As a result, the d_{z^2} -orbital of the central Pd atom plays an important role in the structure of these Pd complexes.

The potential energy surfaces for the ligand exchange processes involving the reactant $\{(PdZ_2Cl_2 \cdots H_2O; Z = NH_3, PH_3), \mathbf{A}\}$, the transition state $\{([PdZ_2Cl]^+ \cdots [H_2O][Cl^-])^\ddagger, \mathbf{B}\}$, and the product $\{([PdZ_2Cl(H_2O)]^+ \cdots Cl^-), \mathbf{C}\}$ proceed *via* both hydrogen-bonded and direct $(Pd \cdots H_2O)$ interactions. Each reaction surface has one transition state $(PdZ_2Cl]^+ \cdots [H_2O][Cl^-])^\ddagger$ complex with a 6-membered ring such as $(Pd-OH \cdots Cl \cdots HN)$ and $(Pd-OH \cdots Cl \cdots HP)$. In the transition state, the central Pd(II) cation interacts with a departing Cl^- and an entering H_2O , and the entering H_2O

simultaneously interacts with a departing Cl^- . The fifth H_2O ligand axially approaches the central Pd cation on the square planar Pd complexes. The vertical interaction between the d -orbital of Pd(II) and the lone pair electron of the fifth H_2O ligand is strong due to the π -back donation from the Pd(II) center to the P atom of PH_3 and the departure of the negatively charged Cl^- anion. As a result, the reaction mechanisms for the ligand exchange reactions from $(Pd(PH_3)_2Cl_2 + H_2O)$ to $(Pd(PH_3)_2ClH_2O + Cl^-)$ proceed more apical direction and energetically lower than those from $(Pd(NH_3)_2Cl_2 + H_2O)$ to $(Pd(NH_3)_2ClH_2O + Cl^-)$.

Acknowledgments. This research was supported by a grant (code: F0004021) from the Information Display R&D Center, one of the 21st Century Frontier R&D Programs funded by the Ministry of Commerce, Industry and Energy of the Korean Government.

References

- Blake, A. J.; Holder, A. J.; Hyde, T. I.; Roberts, Y. V.; Lavery, A. J.; Schröder, M. *J. Organomet. Chem.* **1987**, 323, 261.
- Blake, A. J.; Gould, R. O.; Radek, C.; Schröder, M. *J. Chem. Soc. Dalton Trans.* **1995**, 4045.

3. Kozelka, J.; Bergès, J.; Attias, R.; Fraita, J. *Angew. Chem. Int. Ed.* **2000**, 39(1), 198.
 4. Park, J. K.; Cho, Y. G.; Lee, S. S.; Kim, B. G. *Bull. Korean Chem. Soc.* **2004**, 25, 85.
 5. Deeth, R. J.; Elding, L. I. *Inorg. Chem.* **1996**, 35, 5019.
 6. Pavankumar, P. N.; Seetharamulu, P.; Yao, S.; Saxe, J. D.; Reddy, D. G.; Hausheer, F. H. *J. Comput. Chem.* **1999**, 20, 365.
 7. Chval, Z.; Sip, M. *J. Mol. Struct.* **2000**, 532, 59.
 8. Cost, L. A. S.; Rocha, W. R.; De Almeida, W. B.; Dos Santos, H. F. *J. Chem. Phys.* **2003**, 118, 10584.
 9. Park, J. K.; Kim, B. G. *Bull. Korean Chem. Soc.* **2006**, 27, 1405.
 10. Yoon, Y.-J.; Koo, I. S.; Park, J. K. *Bull. Korean Chem. Soc.* **2007**, 28, 1363.
 11. Caminiti, R.; Carbone, M.; Sadun, C. *J. Mol. Liquid* **1998**, 75, 149.
 12. Lienko, A.; Klatt, G.; Robinson, D. J.; Koch, K. R.; Naidoo, K. J. *Inorg. Chem.* **2001**, 40, 2352.
 13. Frish, M. J.; Trucks, G. W.; Head-Gordon, M. H.; Gill, P. M. W.; Wong, M. W.; Foresman, J. B.; Johnson, B. G.; Schlegel, H. B.; Robb, M. A.; Replogle, E. S.; Gomperts, R.; Andres, J. L.; Raghavachari, K.; Binkley, J. S.; Gonzalez, C.; Martin, R. L.; Fox, D. J.; Defrees, D. J.; Baker, J.; Stewart, J. J. P.; Pople, J. A. *Gaussian 03*; Gaussian Inc.: Pittsburgh, 2003.
 14. Becke, A. D. *The Challenge of d- and f-Electrons: Theory and Computation*, ACS Symposium Series, No. 394; Salahub, D. R., Zerner, M. C., Eds.; American Chemical Society: Washington D.C., 1989; p 166; Becke, A. D. *Phys. Rev.* **1988**, A38, 3098; Perdew, J. P. *Phys. Rev.* **1986**, B33, 8822.
 15. Lee, C.; Yang, W.; Parr, R. G. *Phys. Rev.* **1988**, B37, 785.
 16. Roman Boča, *Int. J. Quant. Chem.* **1987**, 31, 941-950.
 17. Ponec, R.; Reřicha, R. *J. Organomet. Chem.* **1988**, 431, 549.
 18. Tondello, E.; Di Sipio, L.; De Michelis, G.; Oleari, L. *Inorg. Chem. Acta* **1971**, 5, 305.
 19. Zeizinger, M.; Burda, J. V.; Šponer, J.; Kapsa, V.; Leszczynski, J. *J. Phys. Chem. A* **2001**, 105, 8086.
 20. Bickelhaupt, M.; Ziegler, T.; Schleyer, P. von R. *Organomet.* **1995**, 14, 2288.
 21. Liao, M.-s.; Zhang, Q.-er. *Inorg. Chem.* **1997**, 36, 396.
 22. Harvey, P. D.; Reber, C. *Can. J. Chem.* **1999**, 77, 16.
 23. Bray, M. R.; Deeth, R. J.; Paget, V. J.; Sheen, P. D. *Int. J. Quant. Chem.* **1996**, 61, 85.
 24. Park, J. K.; Kim, B. G.; Koo, I. S. *Bull. Korean Chem. Soc.* **2005**, 26, 1795.
 25. Allen, F. H.; Kennard, O. *Chem. Des. Autom. News* **1993**, 1, 31.
 26. Bridgeman, A. J.; Gerloch, M. *Mol. Phys.* **1993**, 79, 1195.
 27. Templeton, D. H.; Templeton, L. K. *Acta Crystallogr.* **1985**, A41, 365.
 28. Takazawa, H.; Ohba, S.; Saito, Y. *Acta Cryst.* **1988**, B44, 580.
 29. Bell, J. P.; Hall, D.; Waters, T. N. *Acta Cryst.* **1960**, 21, 440.
 30. Chen, Y.; Christensen, D. H.; Nielsen, O. F.; Hyldtoft, J.; Jacobsen, C. J. H. *Spectrochim. Acta* **1995**, A51, 595.
 31. Valle, G.; Ettore, R. *Acta Crystallogr.* **1994**, C50, 1221.
-